Recent Studies on Diffusion in Intermetallics by Mössbauer Spectroscopy and Nuclear Resonant Scattering of Synchrotron Radiation

Gero Vogl

Institut für Materialphysik der Universität Wien
Strudlhofgasse 4, A-1090 Wien, Austria

(Received December 24, 1997)

ABSTRACT

The extremely high energy resolution of Mössbauer spectroscopy permits the determination of the elementary diffusion jump of iron atoms in crystalline solids. This is accomplished through the interference of γ–radiation emitted from or absorbed at diffusing ^{57}Fe atoms. Measurements at single crystals oriented in different directions relative to the γ–radiation provide information not only on the jump frequency, but also on the jump vector of the diffusing atom. Two intermetallic alloy systems have been studied:

(a) Fe-Al in the composition range between equiatomic stoichiometry (ordered $Fe_{50}Al_{50}$, B2 structure) and $Fe_{72}Al_{28}$ (disordered at high temperature, A2 structure).

(b) Fe-Si at compositions close to Fe_3Si ($D0_3$ structure).

We also report on the first investigations of the elementary diffusion jump in intermetallics with the new method of nuclear resonant scattering of synchrotron radiation. The prospects of this method are that measurements at tiny samples in short times and hopefully even on systems without iron will be possible.

1. INTRODUCTION

The elementary diffusion jump in pure metals and in dilute alloys appears to be well established: in most cases it is a jump into a vacancy on the nearest-neighbour position. For jumps on ordered lattices, an interesting problem arises that has occupied scientists active in the field of diffusion for quite a number of years. In the simplest case the situation is as follows: imagine a cubic structure with two interpenetrating sublattices where the nearest-neighbour sites to any site belong to the sublattice of the other species. Where will an atom jump? Will it overcome the ordering energy and jump to a nearest-neighbour (NN) "antistructure site", i.e. a site belonging to the sublattice of the other species, or will it rather perform direct jumps over a larger distance in order to return directly to its own sublattice? Both alternatives are expensive in terms of energy, i.e., why sophisticated mechanisms have been conceived to induce the correct mechanisms from indirect evidence of tracer diffusion studies /1/. Much theoretical effort has gone into explaining in particular the diffusion jump in alloys with B2 structure.

Mössbauer spectroscopy permits to deduce the elementary diffusion jumps of iron atoms through measuring the angular dependence of the energy broadening ("diffusional broadening") of the Mössbauer line. This has been demonstrated for diffusion of Fe in dilute Al and Cu alloys /2/. Reviews on the potentials and limits of the method in comparison to traditional methods like e.g. measuring penetration profiles by tracer diffusion may be found in Ref. 3. An earlier review on Mössbauer studies of the elementary diffusion jump in intermetallics can be found in Ref. 4.

Closely related to quasielastic Mössbauer spectroscopy is quasielastic neutron scattering, but the energy (i.e. time resolution) of the latter method is worse. For a comparison of the two methods for studying diffusion see, e.g., /5/. The two methods are complementary in that the best suited elements are different: for quasielastic neutron scattering a high incoherent scattering cross-section of the nuclei of the diffusing atom is needed, whereas quasielastic Mössbauer spectroscopy needs "Mössbauer nuclei", as

e.g. ^{57}Fe or ^{119}Sn, and thus has a rather limited range of application.

We have recently reported on a new technique /6/ for determining the elementary diffusion jump in crystalline solids with better angular resolution and in much shorter times than possible before with quasielastic Mössbauer spectroscopy or quasielastic neutron scattering. The method is based on the nuclear excitation of the Mössbauer nuclear level, not by γ–radiation, but rather by highly monochromatized synchrotron radiation. The method instead of studying the energy broadening of the Mössbauer line, follows the intensity decay of nuclear resonant scattering of synchrotron radiation (NRSSR) in forward direction over a time interval in the order of the life time of the Mössbauer level (here the 14.4 keV level of ^{57}Fe with 140 ns life time) and studies the acceleration of the decay due to diffusion-induced loss of coherency of the scattered radiation. For realising a study with a great number of crystal orientations in limited beamtime we made use of an abbreviated method which time-integrates over the intensity. A diffusionally accelerated decay will lead to a lower integrated intensity than without diffusion.

2. THEORY

Quasielastic Mössbauer spectroscopy examines energy broadening of incoherent atomic motion, in particular diffusion. The elastic line is the resonance line due to nuclear emission or resonant absorption of a gamma quantum. The emission or absorption probability is proportional to $S(Q,\omega)$, the double Fourier transform of the self-correlation function $G_s(r,t)$ /7,8/ from space r and time t into momentum transfer $\hbar Q$ and energy $\hbar\omega$

$$S(Q,\omega) \propto \int \exp\left[i(Qr-\omega t)-\Gamma_0 |t|/2\hbar\right]\cdot G_s(r,t)\,dr\,dt \qquad (1)$$

Γ_0 is the natural line width of the Mössbauer transition. In equ. (1) we have omitted all numerical and geometrical factors not relevant for diffusion. The formula indicates that the shape of $S(Q,\omega)$ as a function of the energy difference $\hbar\omega$ between source and absorber and of the direction of the γ-wave vector Q relative to the crystal orientation will depend on the diffusing atom's displacement in space and time. After the Fourier transform one arrives at a Lorentzian line.

Motions on a time scale longer than ten microseconds (taken ^{57}Fe as a reference) do not cause sufficient diffusional line broadening to be visible. Thus, as for many physical methods, we have to do with a limited time window. In terms of the diffusivity D the window corresponds to 10^{-14} m^2/s < D < 10^{-10}m^2/s. This means that sufficiently high diffusivities are needed to see diffusional line broadening.

The essential point of diffusion studies with quasielastic Mössbauer spectroscopy (and also quasielastic neutron scattering) is:
Through its capability to measure the Fourier transform of the self-correlation function of a single atom, Mössbauer spectroscopy (and quasielastic neutron scattering) are without competition in offering a "microscopic" view on the dynamics, whereas the conventional method for measuring diffusion whose general idea is to determine the diffusion profile of tracer atoms yields only the net effect of a great number of jumps and therefore is a macroscopic method. Since Mössbauer spectroscopy measures the self-correlation function in time and space $G_s(r, t)$, from single crystal studies the jump frequency and the jump vector can be derived. Quasielastic Mössbauer spectroscopy is superior to other nuclear methods as NMR or PAC which only can determine $G_s(t)$ that yields only the jump frequency.

Measurements at single crystals (where available) provide maximum information. For metallic systems rather high temperatures are mandatory which demands a special type of furnace. Orientation of the crystal in the furnace is a difficult task and needs an in-furnace goniometer, if possible with a computer steered automatic for changing the crystal orientation.

2.1 Quasielastic Mössbauer spectroscopy for studying diffusion in cubic Bravais lattices

Whereas the Singwi-Sjölander formula (1) applies quite generally to diffusion processes in liquids or solids, Chudley and Elliott /9/ considered the particular case of diffusion jumps in an empty lattice. They wrote down a rate equation for jump diffusion in an *empty* Bravais lattice

$$\frac{\partial P(r,t)}{\partial t} = \frac{1}{N\tau} \cdot \sum_k \left[P(r + l_k, t) - P(r,t)\right]. \qquad (2)$$

P(r ,t) is the probability of finding a diffusing atom at r, which can jump to N sites (index k) in vector distance l_k from r, in the simplest case to a nearest neighbour site.

The diffusional part of the self-correlation function $G_s(r, t)$ is the solution of this equation. Inserting $G_s(r, t)$ into equ.(1) yields a Lorentzian dependence in ω, the width of which is called diffusional line broadening Γ. Chudley and Elliott found

$$\Gamma = (2\hbar/\tau)\,[1 - (1/N)\,\Sigma_k \exp(iQ\,l_k)] \qquad (3)$$

The diffusional line broadening Γ (HWHM) is proportional to the reciprocal of the atom's residence time τ at one lattice site before jumping to any NN site, and is further determined by the sum over a structure factors $\exp(iQl_k)$ of what we call the "jump lattice".

For comparison of the results with results from tracer diffusion studies, it may be instructive to remember that the diffusion constant is given by the Einstein-Smoluchowski equation $D = l^2/6\,\tau$. (Here we have neglected the influence of correlation between jumps, l is the average jump length).

It is evident from what has been said before that maximum information on the diffusion event will be received from studies on single crystals, i.e. why we shall concentrate on these.

2.2 Quasielastic Mössbauer spectroscopy for studying diffusion in ordered intermetallic alloys

The original theory describing jumps in Bravais lattices has been extended to the non-Bravais case by Rowe et al. /10/ for quasielastic neutron scattering and completed by several groups /11/. Randl et al. have recently extended the theory to Mössbauer spectroscopy /12/. We refer the reader to that paper which contains mathematical details too involved for the present review.

Non-Bravais lattices are lattices with more than one atom per unit crystal cell. Such lattices can be described as consisting of several interpenetrating sublattices. The reason for the greater complexity of diffusion in non-Bravais lattices is evident: there are different possible jump paths with different jump frequencies.

In the following we consider a system made up of atoms that jump between the sites of a non-Bravais lattice. Note that the residence time will, in general, be different for the different sublattices. For the sake of simplicity we shall assume that only NN jumps are possible - an extension is straightforward.

As the sites do not form a Bravais lattice, the m inequivalent sites per primitive unit cell have to be labelled and the set of jump vectors for each site will, in general, connect inequivalent sites. Therefore, we have to write the jump vectors with more indices than above. Let l_{ij}^k be the vector from the site of local symmetry i to the k-th site of local symmetry j and c_j the probability of occupation of the j-th sublattice. Let further on each site of the i-th sublattice be surrounded by n_{ij} sites of the j-th sublattice.

Now the rate equations are

$$\frac{\partial P_i(r,t)}{\partial t} = \sum_{j,k} \left[\frac{P_j(r + l_{ij}^k, t)}{n_{ji} \cdot \tau_{ji}} - \frac{P_i(r,t)}{n_{ij} \cdot \tau_{ij}} \right]. \qquad (4)$$

The self-correlation function $G_S(r,t)$ is now a weighted sum of the solutions of the rate equations - compare equ. (5) of /12/ -, therefore $S(Q,\omega)$ is made up of m Lorentzian functions instead of just one:

$$S(Q,\omega) = \sum_p w_p(Q) \frac{\Gamma_p(Q)}{(\Gamma_p(Q))^2 + \omega^2}. \qquad (5)$$

The halfwidths (HWHM) $\Gamma_p(Q)$ of the Lorentzians are the eigenvalues of a matrix **A**, the weights w_p are given by

$$w_p = \left| \sum_i \sqrt{c_i}\, b_i^p \right|^2 \qquad (6)$$

where b_i^p is the i-th component of the p-th eigenvector of matrix **A** belonging to the p-th eigenvalue.

Since **A** describes the jumps between various sites, we call **A** the "jump matrix". The elements of matrix **A** are

$$A_{ij} = \frac{1}{n_{ji}.\tau_{ji}} \cdot \sum_k \exp(-iQl_{ij}^k) - \delta_{ij} \cdot \sum_j \frac{1}{\tau_{ij}} \qquad (7)$$

2.3 Nuclear resonant scattering of synchrotron radiation for studying diffusion in ordered intermetallic alloys

To describe the influence of diffusion on the time decay of the nuclear resonant scattered synchrotron radiation intensity, we make the following considerations: In case of diffusive motion which is from its nature a random process, the dephasing of radiation-field components from different atomic sites proceeds faster than in case of atoms on a static lattice. The coherent signal is destroyed, i.e. the diffusional broadening of the Mössbauer line corresponds to a faster intensity decay of the nuclear scattered intensity as compared to the static situation.

According to Kohn and Smirnov /13/ the intensity of NRSSR in forward direction for a sufficiently thin sample is

$$I(t,z) \propto L^2 \exp[(-t/\tau_0)\,[(1 + \Gamma/\Gamma_0 + L/4)] \qquad (8)$$

where t is the time after nuclear excitation by the synchrotron pulse, τ_0 is the nuclear life time connected to the natural line width Γ_0 in Mössbauer spectroscopy, z is the sample thickness, L is the effective dimensionless Mössbauer sample thickness, and Γ the diffusional line broadening in classical quasielastic Mössbauer spectroscopy. The logarithm of the decay rate is now directly proportional to the diffusional line broadening Γ as measured in classical quasielastic Mössbauer spectroscopy.

The intensity decay depends not only on the frequency of the ^{57}Fe jumps, but also on the angle between the beam direction and the jump vector connecting the adjacent lattice sites. This is caused by the different phase-shifts of the resonant X-ray waves from different lattice sites. Again maximum information is therefore obtained from measurements on single crystals.

3. EXPERIMENTAL RESULTS AND INTERPRETATION

3.1 Intermetallic alloy with B2 Structure

3.1.1 Mössbauer spectroscopy of Fe-Al near equiatomic stoichiometry (near $Fe_{50}Al_{50}$) /14/

Ordered Fe-Al has two atoms in its elementary cell, i.e. it has a non-Bravais lattice. Fig. 1 shows Mössbauer spectra for transmission in two particular directions, namely along [113] and [001] at 1065°C. Obviously for each crystal orientation there is *only one* diffusionally broadened Mössbauer line in apparent contrast to the prediction of equ. (5).

Along [001] the Mössbauer resonance is broader than along [113]. The diffusional line broadening is determined by subtracting the natural line width (due to nuclear life time of 14.4 keV Mössbauer level of ^{57}Fe) from the measured line width. Figure 2(a) shows the diffusional line broadening for T = 1065°C. Noticeable are the strong minima in [113] and [111] directions.

Fig. 3 shows the results of calculations for iron jumps into a NN antistructure site, along the edge of

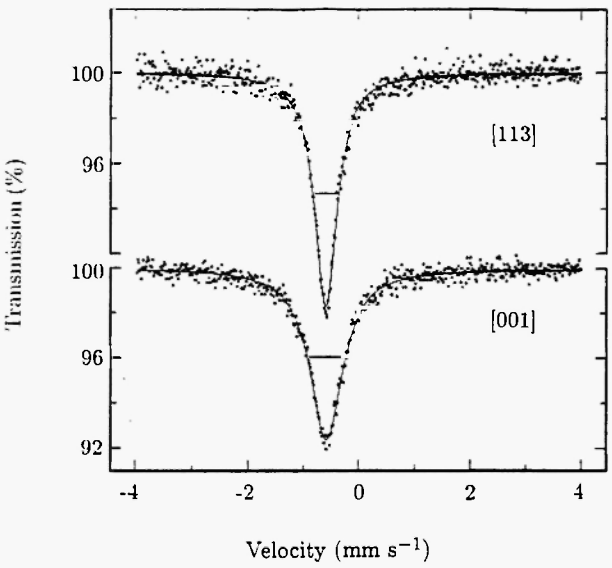

Fig. 1: Mössbauer spectra of ^{57}Fe in $Fe_{50.5}Al_{49.5}$ along [113] and [001] direction. Velocity scale relative to α-Fe, measuring temperature 1065°C.

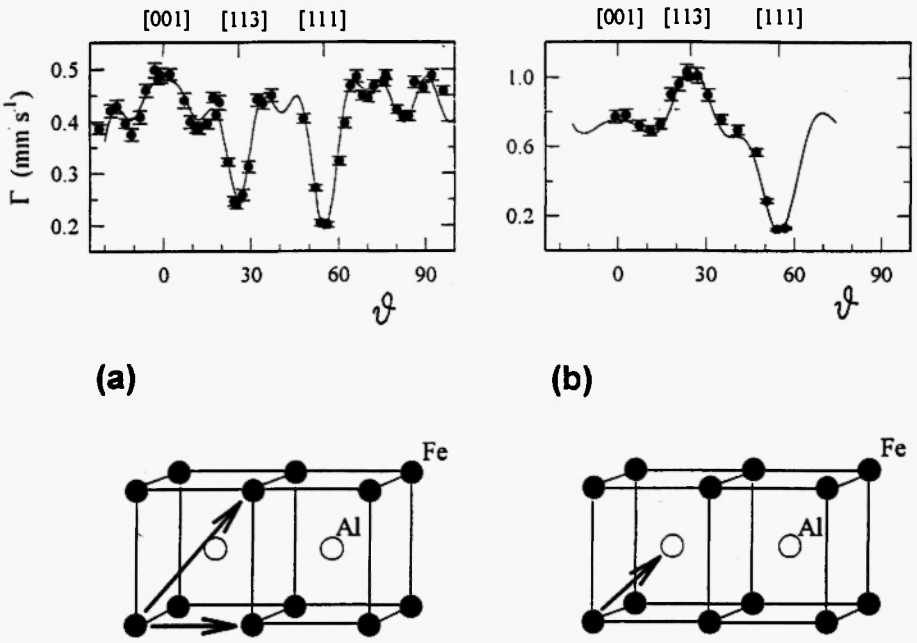

Fig. 2: ***Top figures:*** (a) Equiatomic ordered FeAl. Diffusional line broadening as a function of direction of γ-transmission. ϑ is the angle in the (110) measuring plane. Symbols: experiment $Fe_{50.5}Al_{49.5}$, T=1065°C. For explanation of solid line (model) see text. (b) The same for disordered $Fe_{72}Al_{28}$.
Bottom figures: Scheme of jump(s) into a NN vacancy in (a) ordered stoichiometric FeAl and (b) in the disordered Fe-Al alloy.

the cubic unit cell ([100] direction), via its face diagonal ([110] direction) and via its body diagonal ([111] direction). One recognizes that each model curve alone is inappropriate for fitting the experimental data. The following superposition, however, gives a good fit:

$$\Gamma(Q) = (2\hbar/\tau)\,[1 - \Sigma_j W_j\,(1/N_j)\,\Sigma_n \exp(iQl_n)], \qquad (9)$$

where $1/\tau$ is the jump frequency between lattice sites, W_j is the probability for a particular type of jump (e.g. to nearest neighbours, second nearest neighbours etc.) and $\exp(iQl_n)$ is a structure factor with l_n ($n = 1$ to N_j) the N_j possible jump vectors from one lattice site to another one on the neighbour shell j.

The following observations are made when comparing the measured angular dependence of the line broadening [Fig. 2(a)] and calculated curves. It is obvious that the experimental curve is far from agreeing with Fig. 3 for jumps to NN sites: the model predicts a maximum in direction [113] rather than the minimum found experimentally.

Best fit is received with a ratio (fraction of [110] jumps W_{110}) / (fraction of [100] jumps W_{100}) = 1.7 according to the solid line in Fig. 2. This implies that about 35% of all Fe jumps end up at a second neighbour site and 65% at a third neighbour site.

The central question to be answered when constructing a model for the jump mechanism is: How can one understand that [110] jumps, i.e. third neighbour jumps, are more frequent than [100] jumps, i.e. second neighbour jumps? In the following we examine and compare various jump mechanisms in search for an answer.

Direct jumps to second and third neighbours on the Fe sublattice. A similar or even higher fraction of jumps directly to third neighbours than to second neighbours is hardly conceivable, therefore a simple minded model of this type can certainly be excluded.

Six-jump cycle. Several authors have considered the so-called six-jump cycle as the mechanism for jumps in

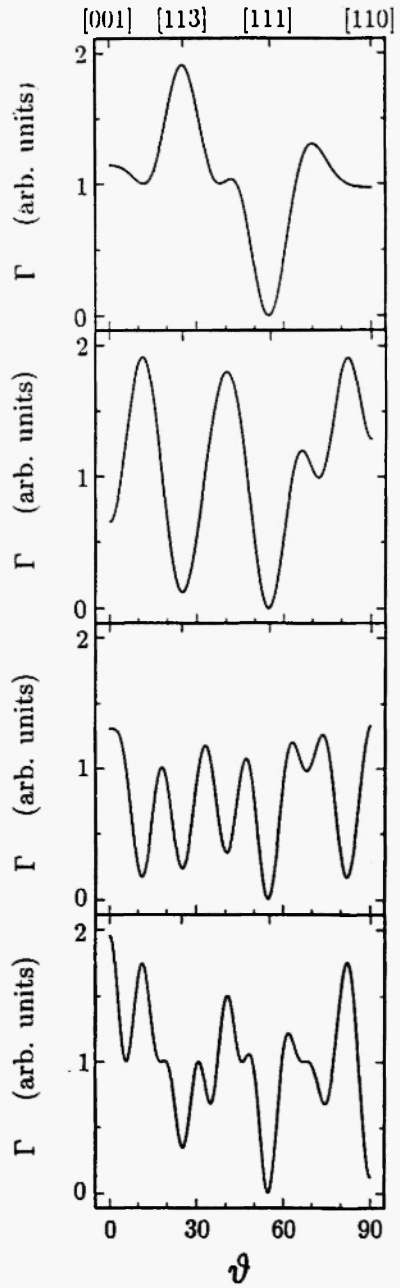

Fig. 3: Expected angular dependence of diffusional line broadening according to equation (3). From top to bottom:
[½ ½ ½] jumps, i.e. to NN sites on the other (Al) sublattice of a B2 lattice with lattice constant a.
[100] jumps, i.e. on a simple cubic lattice with lattice constant a.
[110] jumps, i.e. on a f.c.c. lattice with lattice constant 2a.
[111] jumps, i.e. on a b.c.c. lattice with lattice constant 2a.

B2 lattices. With that mechanism a single vacancy suffices to lead a jumping atom back to its own sublattices after six jumps through intermediate higher-energy states. Arita et al. /15/ have performed thorough calculations finding that the six-jump cycle demands a probability ratio of [110] and [100] jumps between 1/3 and 1. This ratio cannot be reconciled with the ratio $W_{110}/W_{100} > 1.7$ found in the present work which means that based on these calculations we can exclude a significant contribution of the six-jump cycle for diffusion in ordered nearly equiatomic FeAl.

Jumps via a double vacancy, i.e. jumps via antistructure sites on the Al sublattice

A further possibility are jumps via *short-time production of an antistructure defect*, i.e. an Fe atom on the Al sublattice. How that can be imagined is shown in Fig. 4.

It is evident that jumps via antistructure sites can indeed favour [110] over [100] displacements provided there is a tendency of the vacancies on the Fe sublattice to seek optimum distance among each other. We propose vacancies are arranged in a sort of ordered structure, suggestive is a sublattice of the $D0_3$ structure. A jump of an Fe atom will then preferably lead to a site in [110] neighbourhood (because that is a site on the

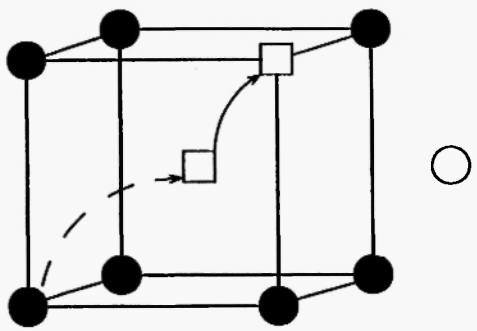

Fig. 4: Jump of Fe atom by help of two vacancies via short time production of antistructure defect. The here drawn jump eventually leads to a displacement of the Fe atom into a third neighbour site in [110] direction. Full circles Fe atoms, open circle Al atom, open squares vacancies, broken arrow slow jump, full arrow fast jump.

same DO_3 sublattice) rather than to a [100] site which is a site on another sublattice.

Fe atom jumps into second or third neighbour sites are jumps on the simple cubic Fe sublattice, with equal occupation of the sites. Jumps to/from the other (Al) sublattice, however, represent a more complicated scenario, i.e. jumps on a non-Bravais lattice. Even though for the Mössbauer spectrum the short intermediate residence of the Fe atom on the Al sublattice is of nearly no importance, since mainly that part of the γ-radiation contributes which is absorbed during the long-term stay of the Fe atom at the start and at the stop sites, an exact treatment demands to apply equations (5) to (7), i.e. the system of coupled rate equations for jumps between the two sites, namely a site at the corner of the cube in Fig. 4 and that in the centre of the cube.

For the present case of a B2 elementary cell containing two atoms and neglecting jumps other than to NN sites we have only two residence times in equ. (4): τ_{12} for Fe atoms on sites on the Fe sublattice before jumping into a vacancy on a distinct NN site on the Al sublattice, and τ_{21}, the residence time of the Fe atom on the Al sublattice before jumping to the Fe sublattice. From detailed balance it follows that in the stoichiometric alloy the ratio of the residence times equals the ratio of the occupancies of the two sublattices c_1 and c_2 by Fe atoms

$$\tau_{12}/\tau_{21} = c_1/c_2 = :\alpha. \qquad (10)$$

Equation (7) describes a 2 x 2 jump matrix A

$$A = \begin{pmatrix} -1 & \alpha \cdot E \\ E & -\alpha \end{pmatrix} \qquad (11)$$

with the structure factor E of the "jump lattice"

$$E = \cos(Q_x a/2)\cos(Q_y a/2)\cos(Q_z a/2), \qquad (12)$$

where Q_x, Q_y, and Q_z are the components of the γ wavevector ($Q = 73\ nm^{-1}$) relative to the crystal axes. The Mössbauer spectrum is expected to be a sum of two Lorentzians.

In particular for short residence time τ_{21} of the iron atom on the antistructure site an additional *very broad* Mössbauer line, weak in intensity, is expected. We were not able to find that line, even when enlarging the energy window (i.e. working with a large velocity of the Mössbauer Doppler drive) and therefore must conclude that the width of the broad line is too large and its intensity too small.

We therefore searched for an angular dependence of the "normal" Mössbauer line as predicted by the model and found an intensity minimum in [113] direction, i.e. exactly where it has to be expected according to the model. The fitted parameter α is about 30 which, due to equation (10) gives an antistructure Fe atoms concentration of about 3%.

It should be pointed out that – even though the picture obtained by quasielastic Mössbauer spectroscopy appears to be consistent – the diffusion mechanism in well ordered equiatomic FeAl is still under discussion. Mayer and Fähnle calculate the probabilities of different types of jumps (W_{100} etc.) by methods basing on ab-initio calculations /16/. Due to their findings, jumps to next nearest neighbours ([100] sites) are energetically favoured over NN jumps. Work is still in progress and further discussion will be necessary.

3.1.2 Mössbauer spectroscopy of off-stoichiometric Fe-Al /17/

As pointed out above, the spectra of an equiatomic near-stoichiometric alloy may seem to consist of one single Lorentzian even though diffusion takes places via NN jumps. As said above, we think that the reason is a high value of α due to the relatively low concentration of antistructure defects. Therefore we raised the amount of excess iron atoms and measured various off-stoichiometric alloys, in particular $Fe_{66}Al_{34}$, which is still B2 ordered but - due to the composition - exhibits a considerable amount of disorder. The spectra of this alloy clearly consist of two Lorentzians, and the complete set of spectra measured at different orientations can only be fitted under the assumption of NN jumps from the iron to the aluminium sublattice and vice versa.

This leads us to a consistent picture of diffusion in $Fe_{1-x}Al_x$ alloys. Starting near the ideal stoichiometric

B2 composition FeAl we find that iron atoms diffuse via NN jumps to antistructure sites with a remarkably *short* residence time on the aluminium sublattice (and hence a large α). With increasing iron content the residence time of iron atoms on the aluminium sublattice increases and thus (at comparable temperatures from 1020°C to 1090°C) the asymmetry parameter α decreases from 30 to 2.45 ($Fe_{50.5}Al_{49.5}$ and $Fe_{65}Al_{35}$, respectively). In disordered Fe_3Al iron should diffuse on a Bravais lattice, i.e. α=1.

We therefore finally studied $Fe_{72}Al_{38}$, an alloy which has no longer B2 structure but in the high temperature range necessary for our studies is disordered (A2). Fig. 2(b) shows the angular dependence of the diffusional broadening of the Mössbauer line /18/. A comparison of figures 2(a) and (b), better than words could do, proves the difference in the elementary jump between the ordered and the disordered state: in the disordered state the angular dependence of the line broadening is indeed nearly perfectly described by a jump into a nearest-neighbour site.

3.1.3 NRSSR study of nearly equiatomic Fe-Al

Very recently time-integrated NRSSR measurements on nearly stoichiometric $Fe_{50.5}Al_{49.5}$ have been performed /19/. Fig. 5 shows values measured at 1030°C, with the sample oriented in 44 different directions. The time integration was from 25 ns to 160 ns after the synchrotron pulse. A very clear angular dependence is obvious. A detailed evaluation follows the same lines as for conventional Mössbauer spectroscopy: Low intensity in NRSSR corresponds to large diffusional broadening in Mössbauer spectroscopy and vice versa.

The agreement with the conclusion from conventional quasielastic Mössbauer spectroscopy as reported above is very good. The angular resolution of NRSSR, however, is by far better than of quasielastic Mössbauer spectroscopy and therefore its reliability is higher.

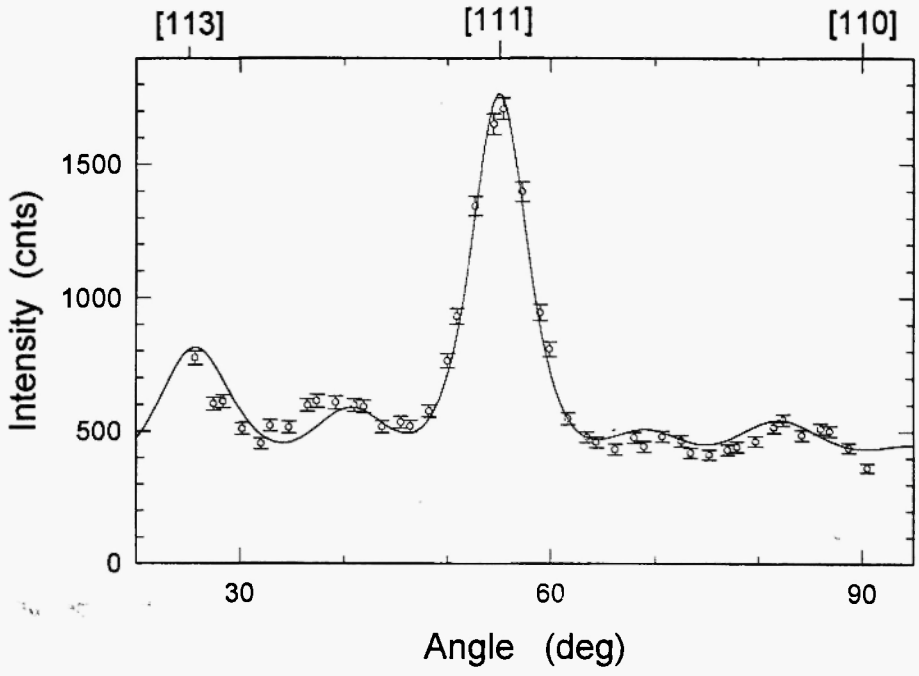

Fig. 5: Angular dependence of integral intensity of NRSSR for 44 orientations from [113] parallel to the beam through [111] to [110]. Symbols: experiment $Fe_{50.5}Al_{49.5}$ T=1030°C. Solid line: same model calculations as for Fig. 2(a).

3.2 Intermetallics with $D0_3$ structure

3.2.1 Mössbauer spectroscopy of Fe-Si close to stoichiometric Fe_3Si /20/

Fe_3Si is an ordered intermetallic alloy and the prototype of the $D0_3$ structure, also named Fe_3Si structure, a cubic superstructure consisting of four sublattices, labelled α_1, α_2, β and γ (Fig. 6).

In the fully ordered structure, the iron atoms occupy the α_1, α_2, and γ sublattices, whereas the silicons occupy the β sublattice. From nuclear Zeeman splitting of Mössbauer spectra we know that order is practically perfect. For non-stoichiometric alloys a distinct component of iron atoms on α sites with five iron NN's appears, and even a small component attributable to iron atoms with six iron NN's can be distinguished. The fractions of these additional components agree with what is expected from statistics.

According to equ. (7), for a model of jumps between the three iron sites, A is a 3x3 matrix:

$$A = \begin{pmatrix} -2 & E & E^* \\ E^* & -1 & 0 \\ E & 0 & -1 \end{pmatrix} \qquad (13)$$

with E the structure factor of the "jump lattice". For the Fe_3Si lattice

$$E = \cos(Q_x a)\cos(Q_y a)\cos(Q_z a) + i\sin(Q_x a)\sin(Q_y a)\sin(Q_z a), \qquad (14)$$

with 4a the lattice parameter (0.571 nm for Fe_3Si at 720°C). The zero values in the matrix indicate that there are no jumps between the α_1 and the α_2 sites, which are further apart than NN.

Now, $S(Q,\omega)$ is a sum of three Lorentzians. Halfwidths of the Lorentzians and weights as predicted by the model are shown in Fig. 7, top. It is evident that for the Mössbauer γ radiation parallel to certain single crystal directions *one* Lorentzian line dominates the Mössbauer spectrum: in [111] it is the narrowest of the three Lorentzians, for [113] it is the broadest one. Measurements should therefore be performed parallel to these directions.

^{57}Fe spectra of Fe_3Si single crystal are shown in Fig. 7 (bottom). A comparison with Fig.7 (top) shows that the model well describes the experimental results: In [111] direction the spectrum can be well represented by just one Lorentzian, whereas the spectrum in [113] direction clearly consists of at least two lines, a narrow one and a broad one. Their fractional intensities are 20% and 80% in agreement with the weights as predicted by the model.

A striking result of these studies was an unusually high diffusivity calculated from the line broadening by help of the Einstein-Smoluchowski equation, a result which has in the meantime been confirmed by tracer studies /21/.

We have also studied how the spectrum changes when the alloy concentration deviates from Fe_3Si stoichiometry /22/. Their surprising result is that already deviations of one to two atomic percent lead to drastic changes which are attributed to a drastic change of the diffusion mechanism.

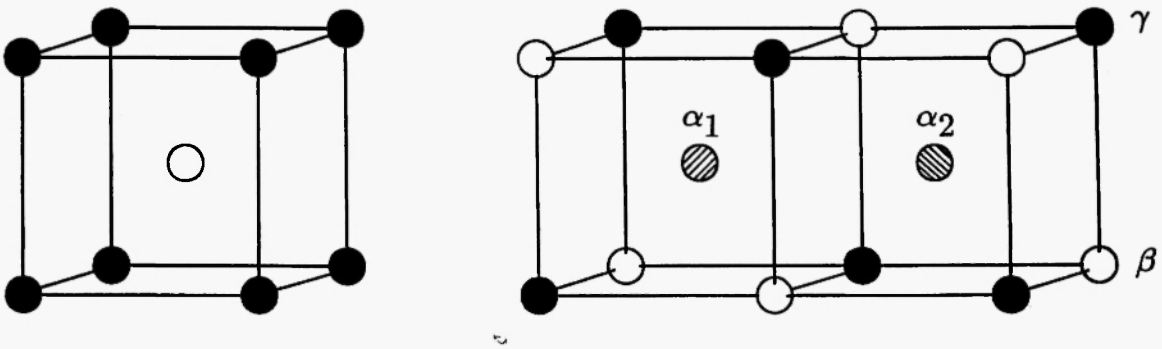

Fig. 6: $D0_3$ structure of Fe_3Si. In the stoichiometric alloy the iron atoms occupy the α_1, α_2 and γ sublattices, the silicon atoms the sublattice ß.

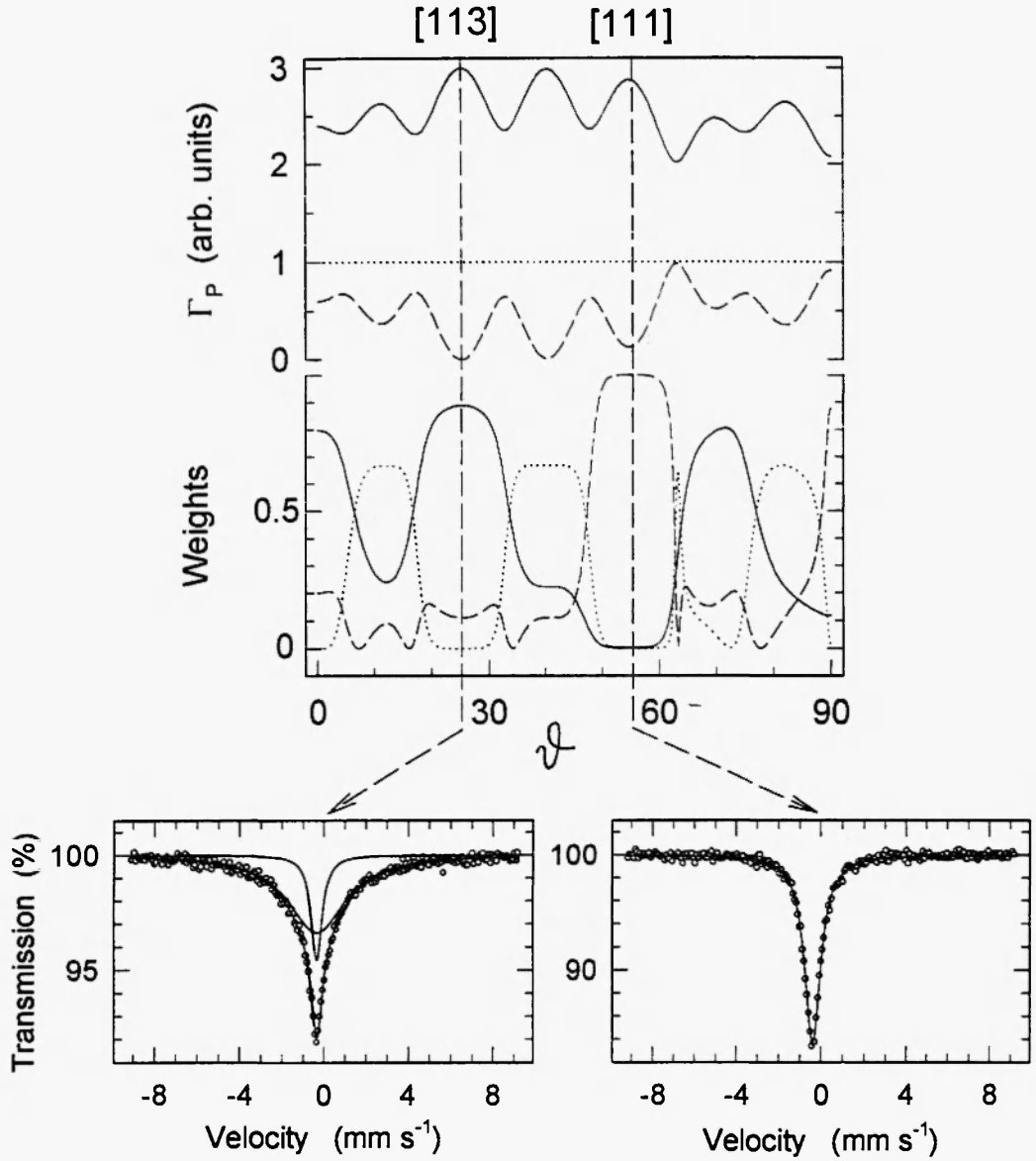

Fig. 7: ***Top:*** Model predictions for linewidths Γ_p and weights w_p of the Mössbauer lines due to diffusion on the three Fe sublattices α_1, α_2 and γ of Fe_3Si, as a function of crystal orientation.
Bottom: Mössbauer spectra along [113] (left) and [111] (right) direction, both at 720°C.

3.2.2 NRSSR study of stoichiometric Fe_3Si

The very first NRSSR measurements ever performed for studying diffusion in a crystalline material have been successfully accomplished on just this model alloy /6/. Fig. 8 shows the time dependence of forward scattered intensity at two different temperatures and directions.

At lower temperatures diffusion is slow and the diffusional acceleration of the intensity decay is rather weak. Beginning from T=827K = 1100°C a difference between the scattering in the [111] and in the [113] direction is observable. At higher temperature a decay with two different rates is clearly visible in the [113] direction. These rates correspond to the narrow and the broad line in the Mössbauer spectrum of the same sample (see figure 7, bottom and /20/). The solid lines

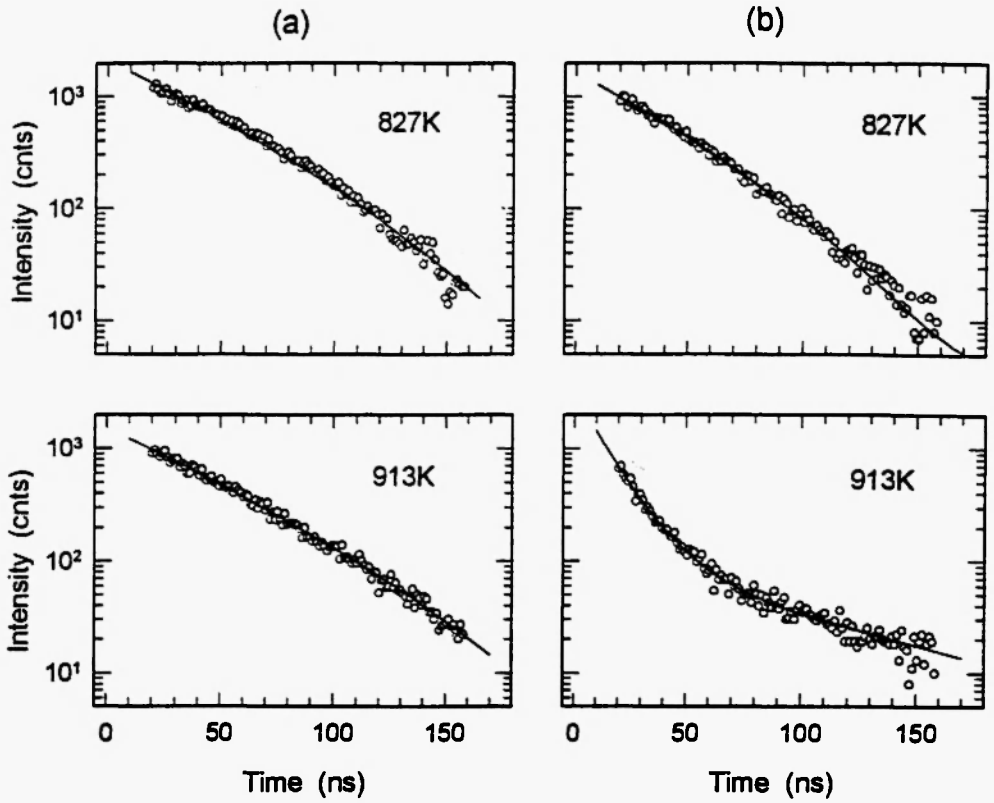

Fig. 8: Nuclear forward scattering of synchrotron radiation measured in (a) [111] and (b) [113] direction at 827K=1100°C and 913K=1186°C. Fits by equ. (8).

are fits using Eq. (8) and the microscopic diffusion model of chapter 3.2.1 allowing jumps of iron atoms between nearest-neighbour iron sites.

We take the opportunity to point out some of the advantages of nuclear resonant scattering of synchrotron radiation compared to conventional quasielastic Mössbauer spectroscopy:

- Diffusion investigations will be orders of magnitude faster than with quasielastic Mössbauer spectroscopy, permitting investigations even at intermetallics which stand high temperatures only for a short time.
- The high brilliance of the synchrotron beam permits diffusion studies on tiny samples (diameter already now less than 1 mm, and probably much less in future) with negligible angular divergence (important for measurements on single crystals under different angles).
- Rayleigh scattering of synchrotron radiation will hopefully remove the present limitation of the measurements to the diffusion of iron atoms.

ACKNOWLEDGEMENTS

I thank B. Sepiol for many enlightening discussions in which he often pointed out problems I had not realized or indicated new ways to go. This work was supported by the Austrian Fonds zur Förderung der Wissenschaftlichen Forschung (Project No. S5601).

REFERENCES

1. M. Koiwa, in: *Ordered Intermetallics Physical Metallurgy and Mechanical Behaviour*, eds. C.T. Liu et al., Kluwer Academic, The Netherlands (1992), p. 449; H. Bakker and D.M.R. Lo Cascio,

Defect and Diffusion Forum 95-98, 803 (1993); H. Mehrer, *Mater. Trans. JIM* 37, 1259 (1996); H. Nakajima, W. Sprengel and N. Nonaka, *Intermetallics* 4, S17 (1996).
2. S. Mantl, W. Petry, K. Schroeder and G. Vogl, *Phys.Rev.* B27, 5313 (1983); K. H. Steinmetz, G. Vogl, W. Petry and K. Schroeder, *Phys. Rev.* B34, 107 (1986).
3. G. Vogl, *Hyperfine Interactions* 53, 197 (1990); G. Vogl, in: *Mössbauer Spectroscopy Appl. to Magn. and Mat. Sci.*, Vol. 2, eds. G. J. Long and F. Grandjean, Plenum Press (1996), p.240.
4. B. Sepiol, *Defect and Diffusion Forum* 125-126, 1 (1995).
5. G. Vogl, *Physica* B226, 135 (1996).
6. B. Sepiol, A. Meyer, G. Vogl, R. Rüffer, A. I. Chumakov and A. Q. R. Baron, *Phys. Rev. Lett.* 76, 3220 (1996).
7. K. S. Singwi and A. Sjölander, *Phys. Rev.* 119, 863 (1960).
8. K. S. Singwi and A. Sjölander, *Phys. Rev.* 120, 1093 (1960).
9. T. Chudley and R. J. Elliott, *Proc. Phys. Soc.* 77, 353 (1961).
10. J. M. Rowe, K. Sköld, H. E. Flotow and J. J. Rush, *J. Phys. Chem. Solids* 32, 41 (1971).
11. I. S. Andersen, A. Heidemann, J. E. Bonnet, D. K. Ross, S. K. Wilson and M. McKergow, *J. Less-Common Met.* 101, 405 (1984); D. Richter, R. Hempelmann and C. Schönfeld, *J. Less-Common Met.* 172-174, 595 (1991).
12. O. G. Randl, B. Sepiol, G. Vogl and R. Feldwisch, *Phys. Rev.* B49, 8768 (1994).
13. G. Kohn and G.V. Smirnov, *Phys. Rev.* B57,5788 (1998), in the press.
14. G. Vogl and B. Sepiol, *Acta metall. mater.* 42, 3175 (1994).
15. M. Arita, M. Koiwa and S. Ishioka, *Acta metall.* 37, 1363 (1989).
16. J. Mayer and M. Fähnle, *Defect and Diffusion Forum* 143-147, 285 (1997).
17. R. Feldwisch, B. Sepiol and G. Vogl, *Acta. metall. mater.* 43, 2033 (1995).
18. R. Feldwisch, Dissertation, Universität Wien, 1996.
19. B. Sepiol, C. Czihak, A. Meyer, G. Vogl, J. Metge and R. Rüffer, *International Conference on the Applications of the Mössbauer Effect ICAME'97*, Rio de Janeiro 1997, to be publ. in *Hyperfine Interactions.*
20. B. Sepiol and G. Vogl, *Phys. Rev. Lett.* 71, 731 (1993).
21. A.Gude and H.Mehrer, *Phil. Mag.* A76, 1 (1997).
22. B. Sepiol and G. Vogl, *Hyperfine Interactions* 95, 149 (1995).